Architecture of Fiber Network: From Understanding to Engineering of Molecular Gels

Rong-Yao Wang,[†,‡] Xiang-Yang Liu,[*,‡] Janaky Narayanan,[‡] Jun-Ying Xiong,[‡] and Jing-Liang Li[‡]

Department of Applied Physics, Beijing Institute of Technology, Beijing 100081, China, and Biophysics and Micro/nanostructures Laboratory, Department of Physics, Block S12, National University of Singapore, 2 Science Drive 3, Singapore 117542

Received: August 8, 2006; In Final Form: October 10, 2006

A new approach of engineering of molecular gels was established on the basis of a nucleation-initiated network formation mechanism. A variety of gel network structures can be obtained by regulating the starting temperature of the sol−gel transition. This enables us to tune the network from the spherulitic domains pattern to the extensively interconnected fibrillar network. As the consequence of fibrous network structure turning, desirable rheological and other in-use properties of the materials can be obtained accordingly. This approach of micro-/nanostructural fabrication may open up a new route for micro-/nanofunctional materials engineering in general.

1. Introduction

Molecular gel formed by the self-organization of low molecular mass organic gelators (LMOGs) belongs to a relatively new class of supramolecular materials.[1−5] It is believed that the formation of LMOG superstructure is mediated solely by noncovalent forces.[4] As a consequence, thermoreversibility is the characteristic feature to distinguish the molecular gels from the covalent force mediated chemical gels. A three-dimensional interconnecting fiber network is the major constituent of the gel superstructure, which entraps the solvent by capillary force to form a viscoelastic soft material. The network microstructure determines the macroscopic property of the material and consequently influences its performance/functionality. For instance, the microstructure of the cytoskeletal network determines the mechanical property of the cell and influences significantly the cell mobility, mechanoprotection, and division.[6] The mesh size distribution in a drug delivery gel system controls the drug release rate.[7] Engineering of the network structure to modify the macroscopic property is of considerable importance in optimizing the performance of a functional material.

It has been widely accepted that gel network architecture is linked to a hierarchy of self-assembling of molecules. From microscopic scale to macroscopic scale, three levels of structures are recognizable.[2] The aggregation of gelator molecules builds the primary structure. Further unidirectional assembly to form fibrous objects such as rods, tubes, or sheets is the secondary structure. The interconnection of individual fibrous objects leads to the tertiary structure, i.e., the gel network. It has been demonstrated that the primary and secondary structures can be morphologically controlled by proper design and selection of the gelator and solvent molecules.[1,5,8,9] However, controlling the tertiary network structure so as to obtain the desired macroscopic property of a gel material still remains a challenge, due to poor understanding of the transition from individual fibrous assemblies to the network formation.

In this work, the nucleation and growth behaviors in the development of fiber networks of the molecular gel systems are discussed and a strategy for engineering the network structures is proposed in terms of the nucleation-initiated network formation mechanism. Our goal is to explore the method of manipulation of growth modes in order to design gel materials with tunable topological structures and consequently the modified macroscopic properties.

2. Experimental Section

The gelling system studied consists of the LMOG molecule *N*-lauroyl-L-glutamic acid di-*n*-butylamide, GP-1 (>98%, from Aijnomoto), and the solvent propylene glycol, PG (>99%, Cognis). To get the phase diagram of the GP-1/PG system, the measurement of GP-1 solubility in PG was conducted as follows:[10] gels at a series of concentrations C_{eq} in the range from 2 to 6 wt % were prepared in glass tubes and put in a water bath. The temperature at which the last tiny part of gel was completely dissolved was taken to be the equilibrium dissolution temperature T_{eq}.

The GP-1/PG gel is normally turbid, and the microstructure can be visualized by optical microscopy. For optical observation, sample films were prepared by sealing the hot solution of GP-1/PG in glass cells (with a diameter of 5 mm and the spacer thickness of 0.1 mm). A conventional microscope (Olympus BX50) with a heating/cooling temperature controller (Linkam Scientific Instrument, THMS600) at the sample stage was used. The temperature ramp could be varied from 0.01 to 50 °C/min with an accuracy in temperature of 0.1 °C. The images from the microscope were converted to digital images through a JVC KY-F55B 3-CCD color video camera and analyzed by the acquired image processing software (analySIS 3.2).

Rheological experiments were performed on an advanced rheological expansion system (ARES-LS, Rheometric Scientific) equipped with 25 mm diameter parallel plates geometry. The GP-1/PG gel samples were sandwiched between the two plates with the gap of 0.7 mm. The time sweep experiments were performed to monitor the dynamic viscoelastic moduli during the sol-to-gel transition. The strain and frequency were set as 0.05%, and 1 Hz, respectively, to prevent any major disturbance of the oscillatory shear force on the gelation process.

* To whom correspondence should be addressed. Telephone: +65-68742812. Fax: +65-67776126. E-mail: phyliuxy@nus.edu.sg.
† Beijing Institute of Technology.
‡ National University of Singapore.

10.1021/jp065101j CCC: $33.50
Published on Web 11/30/2006

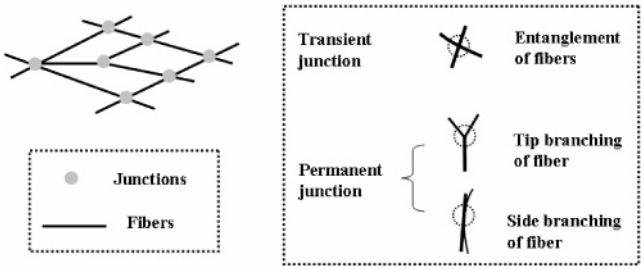

Figure 1. Schematic of fiber network and the nature of junctions. Dashed circles in the right chart denote the sites of junctions.

3. Nucleation and Growth of Fiber Network in the Gelation Process

Topologically, the fiber network structure can be described by the distribution of nodes (junctions) and edges (fibers, which form connection between junctions),[11] as is schematically shown in Figure 1. The junctions, classified as the transient and permanent ones,[4] provide rigidity to the gel microstructure. From the microscopic images of the gel network,[10,12,13] either on nanometer or micrometer resolution, two types of junctions (Figure 1) are usually seen: One is the entanglement of fibers,[10,12] which is of transient nature. The other is the branching of fibers, including the side-branching and tip-branching from the growing fibers.[10,13] These are permanent junctions that are prevalent in a strong gel network.

The formation mechanism of a molecular gel has been understood recently in terms of the nucleation and growth of a gel network. By using multiple techniques to investigate the nucleation and growth kinetics of a molecular gel network, Terech et al.[14] have demonstrated that the gelation occurs via instantaneous nucleation and the one-dimensional growth of fibers. This result is consistent with the model of the self-assembled fibrillar network,[2,8] which is referred to as the fibrous growth model. According to this model, the formation of a network is mediated mainly through the entanglements of fibers.

On the other hand, the studies made by Fages and co-workers[13] and Liu and co-workers[15] suggested that, subsequent to the primary nucleation and one-dimensional growth of individual fibers, branching of the fibers would be an alternative way to initiate the formation of a tertiary network structure. The representative example of this case is the spherulitic growth of a network which can be described as follows:[10] Once the stochastic formation of the nucleation sites occurs, spherulites emanate radially from each central nucleation site via alternating fiber growth and branching. The advancing growth of the spherulite looks like a propagating wave extending from each center site to the surrounding medium radially until the neighboring spherulites impinge upon one another, and finally the whole gel network appears as a pattern of spherulitic domains. The spherulite consists of a highly ordered structure of fiber arrays, showing birefringence (Maltese Cross extinction pattern[16]) under polarized light microscopy.

Supersaturation-driven crystallographic mismatch branching (CMB,[15] also called noncrystallographic branching[17]) is believed to be a new mechanism governing the nucleation and growth of a gel network. According to the CMB model,[15] the branching either on the side surface or at the tip of a growing fiber originates from crystallographic mismatch nucleation, i.e., the secondary nucleation, and the mismatch nucleation rate J at the surface of a fiber can be expressed as[15]

$$J = f'[f]^{1/2} B \exp\left[-\frac{\Delta G^*_{\mathrm{mis}}}{kT}\right] \tag{1}$$

with

$$\Delta G^*_{\mathrm{mis}} = \frac{16\pi\gamma_{\mathrm{cf}}{}^3\Omega^2}{3(kT)^2[\Delta\mu/kT]^2} f \tag{2}$$

$$\Delta\mu/kT = \ln(1+\sigma) \cong \frac{\Delta H_{\mathrm{diss}}}{kT_{\mathrm{eq}}T}(T_{\mathrm{eq}} - T) \tag{3}$$

where $\Delta G^*_{\mathrm{mis}}$ is the crystallographic mismatch nucleation barrier, B is the kink kinetics coefficient, f'' and f ($f'' \le 1$, $f > 0$) are the factors describing the correlation between the substrates and the nucleation phase, k is the Boltzman constant, Ω is the volume of growth units, γ_{cf} denotes the interfacial free energy of the fibers and the fluid phase, ΔH_{diss} denotes the molar dissolution enthalpy of the nucleating phase, T_{eq} is the equilibrium dissolution temperature, $\Delta\mu$ denotes the chemical potential difference between gelator molecules in fiber and in liquid, and σ is supersaturation, defined as $\sigma(T) = (C - C_{\mathrm{eq}}(T))/C_{\mathrm{eq}}(T)$, where C and $C_{\mathrm{eq}}(T)$ are respectively the actual molar fraction and the equilibrium molar fraction of solute in solution at temperature T.

From eq 1, one can understand that, similar to normal nucleation, the kinetics of crystallographic mismatch nucleation depends on the supersaturation at the surface of the growing crystal,[15,17] and its rate increases monotonically with the bulk supersaturation in the system. Therefore the induced branching behavior is supersaturation-dependent. Under very low supersaturation condition, branching is difficult due to the crystallographic mismatch nucleation barrier ($\Delta G^*_{\mathrm{mis}}$) being very high. Fiber will grow without branching. As supersaturation increases, $\Delta G^*_{\mathrm{mis}}$ will drop rapidly, and the interfacial structural match between the substrate and the nucleating phase will deviate from the optimal structural match position. Once the crystallographic mismatch nucleation occurs at the growing fiber surface, the growth of the branch from the nucleation site will proceed soon.

Given that growth kinetics of fibers is controlled by the rough growth model, the average branching distance can be expressed as[15]

$$\langle\xi\rangle \sim \frac{A(\Delta\mu/kT)}{f''f^{1/2}} \exp\left\{\frac{16\pi f}{3(\Delta\mu/kT)^2}\left[\frac{\gamma_{\mathrm{cf}}\Omega^{2/3}}{kT}\right]^3\right\} \tag{4}$$

where A is a coefficient associated with volume transport. In principle, the branching rate is proportional to the crystallographic nucleation rate, which suggests that the higher the supersaturation, the higher is the branching frequency (or the shorter the length of branch).

Provided that the gelation time t_g is predominantly determined by the induction time of nucleation in the gelation process, we should have $t_g \sim 1/J$. According to the branching (nucleation) initiated gelation mechanism described by eqs 1−4, we should experimentally observe a linear relationship between $\ln(t_g)$ and $1/[T(\Delta T)^2]$ and also between $\ln[\langle\xi\rangle/(\Delta\mu/kT)]$ and $1/(\Delta\mu/kT)^2$.

These linear relationships have been experimentally examined in several gelling systems,[15] where the gelation kinetics and the fiber network structure under different supersaturation conditions were investigated by the dynamic rheological measurements combined with the microscopic imaging. For the GP-1/PG gelling system used in this study, as shown in Figure 2, a linear relationship is also obtained in the plots of $\ln(t_g) \sim 1/[T(\Delta T)^2]$ and $\ln[\langle\xi\rangle/(\Delta\mu/kT)] \sim 1/(\Delta\mu/kT)^2$, verifying the branching (nucleation) initiated gelation mechanism. t_g is measured from the time evolution of storage modulus G' as shown in the inset

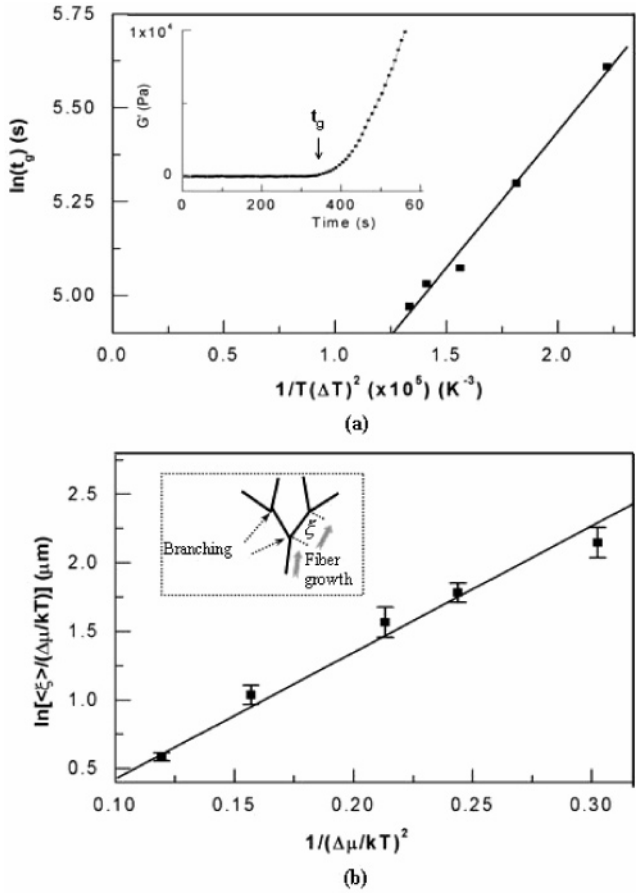

Figure 2. Plots of (a) $\ln(t_g) \sim 1/[T(\Delta T)^2]$ and (b) $\ln[\langle\xi\rangle/(\Delta\mu/kT)] \sim 1/(\Delta\mu/kT)^2$, for the 3 wt % GP-1/PG system. Solid lines are the linear fits of the experimental data.

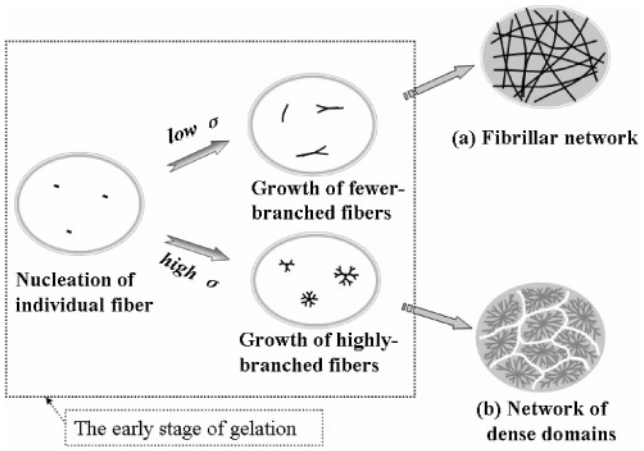

Figure 3. Schematic of the physical process to develop a gel network through (a) the fibrous growth mode and (b) the spherulitic growth mode.

of Figure 2a. The average branching distance ξ is measured from the microscope images.

4. Strategy To Manipulate the Growth Modes of the Gel Network

On the basis of the branching (nucleation) initiated gelation mechanism, the basic physical process involved in the fibrous growth or the spherulitic growth of a gel network can be illustrated as in Figure 3. After the nucleation of individual fibers, (a) under low supersaturation condition (low σ), fibers grow one-dimensionally with less branching and the interpenetration and entanglement of less-branched fibers results in the formation of the fibrillar network, and (b) under high supersaturation condition (high σ), growth of highly branched fibers is facilitated. The densely branching morphology (typically through the spherulitic growth) gives rise to the formation of highly branched fiber arrays (spherulitic domains).

In our previous work,[10] the correlation between the growth modes of a gel network and the supersaturation-dependent branching behaviors (Figure 3) has been experimentally confirmed, especially at the early stage of gelation, through an in-situ investigation of the growth of a gel network. Our results demonstrated that the supersaturation condition, particularly the degree of supersaturation at the early stage of gelation, is a key factor that determines the topological structure of a gel network.[10]

The basic strategy to engineer gel network structure is proposed here in terms of the above understanding of the branching (nucleation) initiated gelation mechanism. From Figure 3, we find that the early stage of gelation, namely, the stage at which the primary nucleation is immediately followed by fiber growth and branching, would play a crucial role in determining the growth modes of a gel network. How to regulate the nucleation and growth behaviors at the early stage of gelation is therefore a key issue. We address this issue and explore an approach that can be used to manipulate the growth modes of a fiber network and engineer the topological structure and consequently the macroscopic property of molecular gel materials.

Unlike the usual thermal protocols where regulation of the gelation (final) temperature[14] and/or the cooling rate[18] are used to modify the structure of the gel network, in the method explained here, the starting temperature of sol−gel transition is regulated while the gelation (final) temperature and the cooling rate are held constant. With this method, the primary nucleation at the early stage of gelation can be selected to be self-seeding or the usual homogeneous or heterogeneous nucleation.

The principle of self-seeding has been well-established:[16] On heating a pre-formed crystal phase sufficiently slowly, the solution will appear macroscopically and microscopically clarified at a particular temperature, the so-called clearing temperature T_{clear}. At such a temperature, it is very likely that a lot of nuclei can survive. The number of the survived nuclei is determined mainly by the rate of heating, the concentration, and the temperature of the initial crystallization.[16] On heating to a higher equilibrium dissolution temperature T_{eq}, all nuclei would disappear, if kept at T_{eq} for long enough time.

A similar physical process may exist in the thermoreversible molecular gel system. Figure 4 illustrates the process of gel-to-sol transition monitored using a rheology parameter. On heating a pre-formed gel phase, the gel melts slowly with the change of the rheological property (e.g., decrease of the storage modulus) and finally transforms into the sol phase. If the pre-formed gel phase is heated from T_g (the gelation temperature) to T_{eq} or above, so that all nuclei are dissolved, the initiation of new gelation would be dominated by the homogeneous or heterogeneous nucleation in the sol phase. On the other hand, if the pre-formed gel phase is heated to a temperature between T_{clear} and T_{eq}, some nuclei would survive, and the initiation of new gelation can be dominated by self-seeding.

Obviously, self-seeding enables the development of a network at a relatively lower supersaturation due to the primary nuclei being already present at the starting temperature (between T_{clear} and T_{eq}) of gelation. On the other hand, the conventionally used

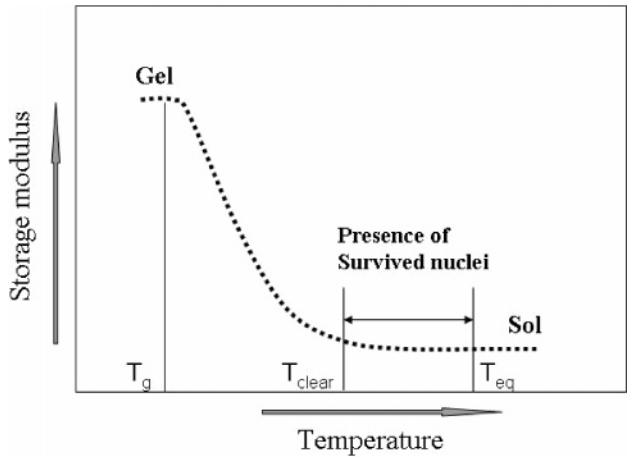

Figure 4. Schematics of the physical process of self-seeding in a molecular gel.

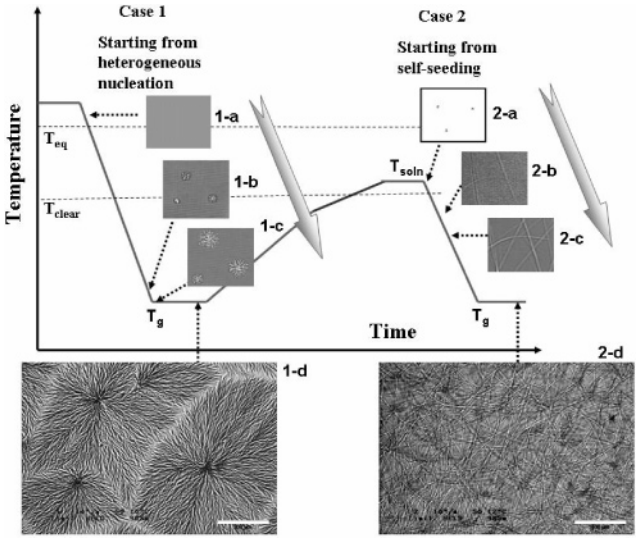

Figure 5. Switching the gel network from spherulitic domains pattern to fibrillar network in a 3 wt % GP-1/PG system. The time/temperature dependence of the network structural evolution during the corresponding thermal control is illustrated in each case. The details are given in the text. The scale bar is 200 μm in 1-d and 100 μm in 2-d.

method that quenches the hot solution from above T_{eq} to T_g is able to produce a condition of higher supersaturation that can initiate the primary homogeneous or heterogeneous nucleation. From eq 3, the larger the difference between starting and quenching (gelation) temperatures, ΔT, the higher is the supersaturation σ. Thus, controlling the primary nucleation condition at the early stage of gelation enables us to regulate the supersaturation for the subsequent growth of the fiber network.

In this work, the initial temperature of the solution T_{soln} was regulated in the range from T_{clear} to above T_{eq}. The subsequent cooling rate and gelation temperature were kept constant in each case. By using the method described in our previous work,[10] T_{eq} and T_{clear} were estimated respectively 80 and 75 °C for a freshly prepared 3 wt % GP-1/PG gel.

5. Results and Discussion

5.1. Switching from the Spherulitic Domains Pattern to the Fibrillar Network. Figure 5 shows the strategy for successful switching of the structure of the gel network from the spherulitic domains pattern to the fibrillar network. The temperature and time dependence of the structural evolution indicated in the thermal control programs describes the nucleation and growth dynamics that lead to different network architectures.

In case 1, the initial temperature of the solution was kept at 90 °C (10 °C above T_{eq}) for more than 5 min to get a homogeneous solution. Subsequent cooling to the final gelation temperature T_g would result in the heterogeneous nucleation[19] that dominates the early stage of gelation. In the optical microscopy, starting from a homogeneous solution (1-a), the stochastic formation of nucleation sites (1-b) arising from heterogeneous nucleation was seen at a low temperature (close to T_g), followed by the spherulitic growth that emanates from each nucleation site (1-c). Finally the gel microstructure exhibited a pattern of spherulitic microdomains (1-d).

In case 2, the pre-formed gel phase was first heated to T_{clear} (75 °C) at the rate of 10 °C/min, followed by further heating to the solution temperature T_{soln} (77 °C, $T_{clear} < T_{soln} < T_{eq}$) at a rather slow rate (1 °C/min) and then kept at T_{soln} for 1 min. Due to the existence of survived nuclei at T_{soln}, new gelation would be initiated predominantly by self-seeding. From these survived nuclei (2-a), one-dimensional growth of fibers (2-b) was seen at a fairly high solution temperature (not far below T_{clear}), i.e., a quite low degree of supersaturation. With further cooling, branching of the fiber was seen due to an increase in supersaturation. The interpenetration and entanglement of the fewer-branched fibers (2-c) finally led to the formation of the fibrillar network (2-d).

Switching the gel structure from the spherulitic domains pattern to the fibrillar network for the molecular gel system can be achieved in another way. Terech et al.[14] obtained the spherulitic domains pattern at the normal gelation temperature, which changed into the fibrillar network at a very narrow range of higher gelation temperature. As shown in eq 3, an increase in the gelation temperature ($T \equiv T_g$) corresponds to lower supersaturation and thus both methods are equivalent. However, in contrast to the method given by Terech et al.,[14] several features of our method can be distinguished: (i) Although formation of the fibrillar network is still limited to a narrow range of solution temperature (see Figure 6), it can be obtained at the normal T_g. (ii) The switch over from the spherulitic domains pattern to the fibrillar network is reversible when cycled through the thermal controls shown in Figure 5. (iii) As shown below, our method provides a simple but practical way of tuning the gel network to a variety of structures intermediate to the spherulitic domains and the fibrillar network. In this regard, our method is more general in engineering the gel network architecture.

The fibrillar network and the spherulitic domains pattern exist ubiquitously in many molecular gels[10,12−14] and biopolymer gels.[20,21] The occurrence of the fibrous growth or the spherulitic growth in some biopolymer systems is closely related to the bioactivity, even the pathogenic consequence.[21] Our study on the manipulation of the growth modes of fiber network in the molecular gel system may help in the understanding of the complicated origins of the nucleation and growth behaviors in the biopolymer systems.

5.2. Structures Intermediate to the Spherulitic Domains Pattern and the Fibrillar Network. By gradually tuning the initial temperature of the solution from above T_{eq} to that near T_{clear}, structures intermediate to the spherulitic domains pattern and the fibrillar network were accessible. Figure 6 shows the structural evolution of the gel network when tuning the initial solution temperature from 90 to 77 °C. With a decrease in the initial solution temperature, there is a transformation from

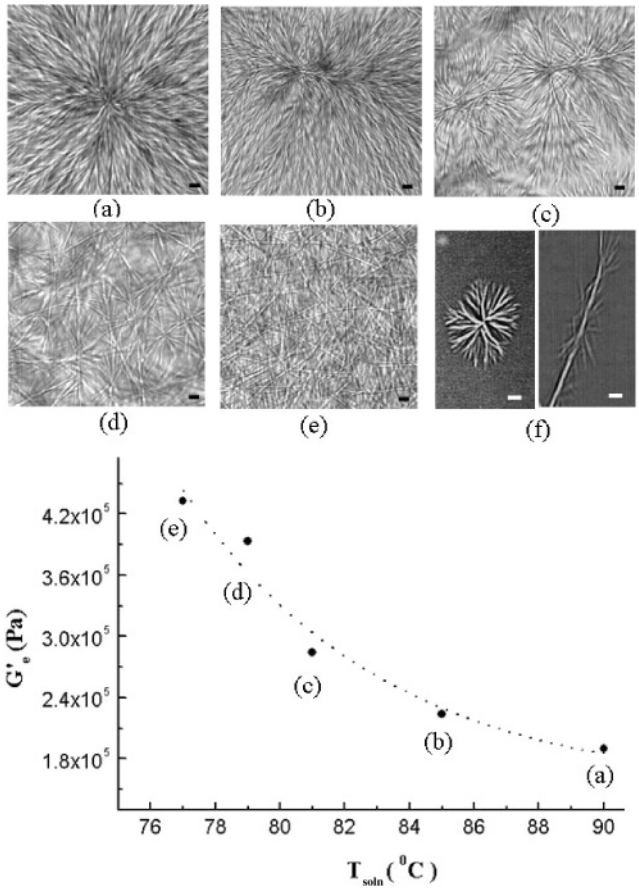

Figure 6. Gel network structure (optical micrographs a−e) and the corresponding rheological property G'_e obtained for the 3 wt % GP-1/PG system by tuning the initial solution temperature T_{soln}. In all cases, the holding time at T_{soln} is 1 min, and the gelation temperature and the cooling rate are, respectively, 50 °C and 10 °C/min. G'_e is the plateau value of the storage modulus. The dotted line is the guide line for showing the enhancement of G'_e when the network structure evolves from the spherulitic domains pattern to the fibrillar network. (f) Tip-branching (left) and side-branching (right) observed in the growth of networks. (Scale bars: 10 μm.)

predominantly spherulitic domains structure (Figure 6a,b) to predominantly fibrillar network structure (Figure 6e). One can see that the formation of the intermediate structures is correlated to the change of the growth modes of the gel network. The intermediate structures (Figure 6b−6d) arise from different contributions from these two growth modes, showing obviously the dependence on the initial solution temperature.

It is worth noting that the density of the nuclei at the early stage of gelation can be another important factor in determining the final topological structure of the gel network. The heating rate, or the time taken to rise to and to hold at the temperature T_{soln}, can give rise to a change in the self-seeding density.[16] More efforts are needed to investigate both experimentally and theoretically the correlation between the self-seeding density at the early stage of gelation and the final topological structure of the gel network. From our preliminary experiments reported here, it is anticipated that a variety of the gel network structures would be produced by controlling the density of the nuclei at the early stage of gelation.

Figure 6 also shows a change of the branching behavior and hence the development of different structures of the gel network. Two typical branching behaviors, i.e., the tip-branching and the side-branching from the growing fibers, were clearly seen in the formation of gel networks (Figure 6f). As the tip-branching transforms through the side-branching into the entanglement, the gel network evolves from the spherulitic domains pattern through the intermediate state into the fibrillar network.

We further examine the rheological property of the corresponding gel in response to the structural changes discussed above. We emphasize here the effect of tuning the topological structure on the mechanical property of a gel network. Since identical gelation temperature is used in each case, the total fiber mass of the gel network can be regarded as constant, regardless of its topological structure. From the plot G'_e versus T_{soln} in Figure 6, one can see a 2-fold increase in the storage modulus when the structures change from a spherulitic domain pattern to a fibrillar network. A quantitative understanding of the structure−property correlation in the molecular gel is still lacking, although it is well-known that the mechanical properties of the gel network depend on multiple factors,[22] such as the thickness and density of fibers, and the nature and distribution of the junctions.

6. Conclusions

In summary, we have demonstrated that tuning of the starting temperature of the sol−gel transition can be used to regulate the nucleation and growth behaviors at the early stage of gelation and hence to manipulate the growth modes of the fiber network, so as to fabricate a molecular gel with tunable structure. We hope that this work may provide a general strategy for engineering self-organized fiber network architectures and consequently modifying the mechanical property of the supramolecular functional materials.

Acknowledgment. We thank Dr. C. Strom for her valuable discussion and kind assistance.

References and Notes

(1) Araki, K.; Brizard, A.; Fages, F.; Hirst, A. R.; Huc, I.; Kato, T.; Kitamura, T.; Liu, X. Y.; Mizoshita, N.; Moriyama, M.; Oda, R.; Smith, D. K.; Vögtle, F.; Yoshikawa, I.; Žinić, M. In *Low Molecular Mass Gelators: Design, Self-assembly, Function*; Fages, F., Ed.; Springer: Berlin, 2005.

(2) Estroff, L. A.; Hamilton, A. D. *Chem. Rev.* **2004**, *104*, 1201−1218.

(3) Hanabusa, K.; Yamada, M.; Kimura, M.; Shirai, H. *Angew. Chem.* **1996**, *108*, 2086−2088.

(4) Terech, P.; Weiss, R. G. *Chem. Rev.* **1997**, *97*, 3133−3160.

(5) Gronwald, O.; Snip, E.; Shinkai, S. *Curr. Opin. Colloid Interface Sci.* **2002**, *7*, 148−156.

(6) Gardel, M. L.; Shin, J. H.; MacKintosh, F. C.; Mahadevan, L.; Matsudaira, P.; Weitz, D. A. *Science* **2004**, *304*, 1301−1305.

(7) Kantaria, S.; Rees, G. D.; Lawrence, M. J. *J. Controlled Release* **1999**, *60*, 355−365.

(8) Simmons, B. A.; Taylor, C. E.; Landis, F. A.; John, V. T.; McPherson, G. L.; Schwartz, D. K.; Moore, R. *J. Am. Chem. Soc.* **2001**, *123*, 2414−2421.

(9) Aggeli, A.; Nyrkova, I. A.; Bell, M.; Harding, R.; Carrick, L.; McLeish, T. C. B.; Semenov, A. N.; Boden, N. *Proc. Natl. Acad. Sci. U.S.A.* **2001**, *98*, 11857−11862.

(10) Wang, R. Y.; Liu, X. Y.; Xiong, J. Y.; Li, J. L. *J. Phys. Chem. B* **2006**, *110*, 7275−7280.

(11) Albert, R.; Barabási, A.-L. *Rev. Mod. Phys.* **2002**, *74*, 47−97.

(12) (a) Geiger, C.; Stanescu, M.; Chen, L.; Whitten, D. G. *Langmuir* **1999**, *15*, 2241−2245. (b) Terech, P.; Allegraud, J. J.; Garner, C. M. *Langmuir* **1998**, *14*, 3991−3998. (c) Wang, R.; Geiger, C.; Chen, L.; Swanson, B.; Whitten, D. G. *J. Am. Chem. Soc.* **2000**, *122*, 2399−2400.

(13) (a) Lescanne, M.; Colin, A.; Mondain-Monval, O.; Fages, F.; Pozzo, J.-L. *Langmuir* **2003**, *19*, 2013−2020. (b) Lescanne, M.; Grondin, P.; d'Aléo, A.; Fages, F.; Pozzo, J.-L.; Monval, O. M.; Reinheimer, P.; Colin, A. *Langmuir* **2004**, *20*, 3032−3041.

(14) Huang, X.; Terech, P.; Raghavan, S. R.; Weiss, R. G. *J. Am. Chem. Soc.* **2005**, *127*, 4336−4344.

(15) (a) Liu, X. Y.; Sawant, P. D.; Tan, W. B.; Noor, I. B. M.; Pramesti, C.; Chen, B. H. *J. Am. Chem. Soc.* **2002**, *124*, 15055−15063. (b) Liu, X. Y.; Sawant, P. D. *Adv. Mater.* **2002**, *14*, 421−426. (c) Liu, X. Y. In *Nanoscale Structure and Assembly at Solid-Fluid Interfaces*; Liu, X. Y., De Yoreo, J. J., Eds.; Plenum/Kluwer Academic: Dordrecht, The Netherlands, 2004; Vol. 1, Chapter 5.

(16) Wunderlich, B. *Macromolecular Physics*; Academic: New York and London, 1973; Vol. 2, Chapter 5.
(17) (a) Khoury, F. *J. Res. Natl. Bur. Stand. Sect. A* **1966**, *A70*, 29−36. (b) Chernov, A. A. *Modern Crystallography III: Crystal Growth*, Springer-Verlag: Berlin, 1984.
(18) (a) Hiroshi, A.; Kikuchi, H.; Hanabusa, K.; Kato, T.; Kajiyama, T. *Liq. Cryst.* **2003**, *30*, 1423−1431. (b) Sawant, P. D.; Liu, X. Y. *Chem. Mater*. **2002**, *14*, 3793−3798.
(19) Liu, X. Y. *J. Chem. Phys.* **2000**, *112*, 9949−9955.
(20) (a) Ferrone, F. A.; Hofrichter, H.; Eaton, W. A. *J. Mol. Biol*. **1985**, *183*, 611−631. (b) Samuel, R. E.; Salmon, E. D.; Briehl, R. W. *Nature* **1990**, *345*, 833−835.
(21) Galkin, O.; Vekilov, P. G. *J. Mol. Biol*. **2004**, *336*, 43−59.
(22) (a) Penzes, T.; Csoka, I.; Eros, I. *Rheol. Acta* **2004**, *43*, 457−463. (b) Shin, J. H.; Gardel, M. L.; Mahadevan, L.; Matsudaira, P.; Weitz, D. A. *Proc. Natl. Acad. Sci. U.S.A.* **2004**, *101*, 9636−9641.